Accepted Manuscript
Version of record at: https://doi.org/10.1016/j.asr.2021.10.045

Comparison of lunar and Martian regolith simulant-based geopolymer cements formed by alkali-activation for in-situ resource utilization

Jennifer N. Mills, Maria Katzarova, Norman J. Wagner*

Department of Chemical and Biomolecular Engineering, University of Delaware, Newark, DE 19716, United States

*Corresponding author
E-mail address: wagnernj@udel.edu (N.J. Wagner)

Abstract
Future human space exploration and habitation on the lunar and Martian surfaces necessitates in-situ resource utilization (ISRU) for the development of construction materials tailored for infrastructure and environmental protection. Here we explore the use of lunar and Martian regoliths to create construction materials with properties suitable for such structures as landing pads. Alkali activation of a spectrum of lunar and Martian regolith simulants generates geopolymer binders under ambient and vacuum curing conditions as well as exposure to extreme high and low temperatures (600 and −80°C). Compressive strength is reduced for binders prepared from each simulant after curing under vacuum and exposure to sub-zero temperatures. In lunar simulant binders, the compressive strength is increased after heating to 600°C, but the opposite effect is observed in the Martian simulant binder. Amorphous aluminosilicate content and percentage of small particles in the simulants are hypothesized to have a positive impact on compressive strength under ambient curing. Iron and magnesium content may be responsible for decreased compressive strength of the Martian binder after heating. This study offers a robust framework for comparing performance of different simulants under the same curing protocols and environmental exposures, as well as offering insight as to the effects of vacuum curing, and exposure to high and low temperature environments on cured binder samples. Developing a landing pad by transporting activator to the lunar surface is shown to be conceptually feasible within current payload constraints.

Keywords
In-situ resource utilization; Regolith simulants

1. Introduction

Building infrastructure on the Moon or Mars is an engineering challenge. The lunar environment cycles from an average of 50 to 202 K (–223 to –71 °C) at the poles (Williams et al., 2017) (the current proposed landing site for Project Artemis is the South Pole (NASA's Plan for Sustained Lunar Exploration and Development, 2020)). Additionally, the lack of lunar atmosphere results in pressures near vacuum, lower protection from solar radiation, and a reduction in gravity to 1/6 that of Earth's. Notably, liquid water, a main component of terrestrial building materials including ordinary Portland cement (OPC), is not stable under these conditions. Furthermore, the cost of sending raw materials into space can be prohibitive. While SpaceX has lowered the payload cost for their launches to low Earth orbit (LEO) to about $850/lb on Falcon Heavy (Seedhouse, 2013), this will become prohibitively expensive when scaling to account for the infrastructure needed to sustain a lunar presence and extending from LEO to lunar or Martian landing, not to mention the physical space required when packing the shuttle. These environmental conditions coupled with payload limitations

Accepted Manuscript
Version of record at: https://doi.org/10.1016/j.asr.2021.10.045

and high cost of sending terrestrial construction materials to space present a challenge for traditional terrestrial methods used for manufacturing building materials. Therefore, there is a critical interest for in-situ resource utilization (ISRU) for future space exploration (Anand et al., 2012; Crawford, 2015; Sanders and Larson, 2012), which extends to developing construction solutions using lunar/Martian regolith in place of terrestrial resources (Khoshnevis et al., 2005; Naser, 2019; Werkheiser et al., 2015).

Lunar regolith is the top several meters of soil layer on the lunar surface, comprised mainly of basaltic and anorthosite rock originating from volcanic flow and broken up by lunar impacts (McKay et al., 1991; Papike et al., 1982). Less is known regarding Martian regolith, but material properties have been studied on the rover missions. As true lunar and Martian regolith samples are not available for widespread use, simulant soils comprised of terrestrial volcanic ash and other natural minerals have been developed and are available for research and development of extra-terrestrial ISRU construction solutions (Allen et al., 1998; Lepper and McKeever, 2000; McKay et al., 1994; Peters et al., 2008; Ramkissoon et al., 2019; Ray et al., 2010; Scott et al., 2017; Stoeser et al., 2010).

Numerous strategies have been considered for extraterrestrial construction (Happel, 1993; Wilhelm and Curbach, 2014). These include traditional OPC-based concrete with lunar regolith as aggregate (Lin et al., 1992; Neves et al., 2020), solar-sintered regolith (Fateri et al., 2019; Imhof et al., 2017; Meurisse et al., 2018), sulfur cement (Khoshnevis et al., 2016; Toutanji et al., 2012; Wan et al., 2016), Sorel cement (Cesaretti et al., 2014; Ordonez et al., 2017; Werkheiser et al., 2015), phosphoric-acid binder cements (Buchner et al., 2018), epoxy/polymer-based cements (Naser, 2019; Naser and Chehab, 2020; Su et al., 2019), and alkali-activated regolith or 'geopolymer'-type binders (Alexiadis et al., 2017; Davis et al., 2017; Montes et al., 2015; Pilehvar et al., 2020; Zhou et al., 2020). In general, the geopolymer binder has the following advantages over the other proposed strategies. The abundant regolith is rich in aluminosilicate minerals but poor in calcium, the latter being critical to OPC, so it is well positioned to serve as the bulk binder starting material. Geopolymers have been prepared at ambient conditions, reducing the energy requirement associated with sintering; the glass transition of JSC-1A lunar regolith simulant is over 600 °C (Ray et al., 2010) and it has been estimated that the energy required to heat 1 m^3 of regolith by 720 °C is on the order of 10^9 J (Crawford, 2015). Sulfur is not abundant on the lunar surface (Haskin and Warren, 1991; Toutanji et al., 2012), so this method may be better served for Martian cements where sulfur is more abundant (Khoshnevis et al., 2016; King and McLennan, 2010). Sorel cement and epoxy/polymer-based systems both introduce the need for additional terrestrial resources for the bulk of the binder, unlike the geopolymer system where the bulk of the binder is the regolith itself. While geopolymers may require some solution to dissolve and activate the regolith, the water demand is much lower compared to OPC (Wang et al., 2017), and water is necessary to be harvested from the polar ice caps for other human sustainability purposes (Li et al., 2018).

While researchers have demonstrated feasibility in producing geopolymer binders using lunar and Martian regolith simulant, much variability exists in simulant type studied- with many researchers developing their own simulants- and limited knowledge as to how these differences may affect binder performance. This study aims to give context for comparing geopolymer binders prepared from different regolith simulants both within lunar simulants and between lunar and Martian simulants.

A second goal of this study was to observe environmental exposure effects on the strength of the binder. Three conditions were chosen: vacuum, sub-freezing temperatures, and high temperatures. Zhou et al. and Pilehvar et al. both note that vacuum studies are a suggested next step in the development of their respective lunar geopolymer studies (Pilehvar et al., 2020; Zhou et al., 2020). Davis et al. specifically studied the effect of vacuum on geopolymer binder prepared from JSC-1A lunar simulant; vacuum curing was seen to decrease compressive strength about 20% at 7 days (Davis et al., 2017). Additionally, C_3S hydration has been studied onboard the international space station, where it was shown that the microgravity environment affected the porosity and phase behavior of the hydrated system (Moraes Neves et al., 2019)- while not the same chemistry as of interest, similar mechanical effects could be possible in lunar geopolymers. Low temperature exposure and thermal cycling have been included in a few studies of lunar geopolymers; both Pilehvar et al. and Wang et al. found freeze-thaw cycling to decrease the compressive strength of their samples (Pilehvar et al., 2020; Wang et al., 2016). Curing at elevated temperatures (ranging up to $\sim$ 90 °C, as may be relevant to daytime lunar surface temperatures) is well documented for geopolymers and shown to affect kinetics, microstructure development, and material strength (D Hardjito et al., 2004a; Muñiz-Villarreal et al., 2011; Rovnaník, 2010; Swanepoel and Strydom, 2002).

One notable requirement for extra-terrestrial cement is the development of vertical takeoff/vertical landing (VTVL) pads for the lunar and Martian surfaces to protect rockets from dust and debris (Gelino et al., 2021). This application will expose the cements to extremely high temperatures. While it was not feasible to test our binders using a true ignition such as has been done by Kelso et al. (Kelso et al., 2016), this study sought to compare the performance and structure of the binders at elevated temperatures. Kong and Sanjayan have demonstrated that while OPC paste may fail at temperatures of 400 °C, fly ash geopolymers were suitable up to 800 °C (Kong and Sanjayan, 2010). Sturm et al. also demonstrated the onset of structural breakdown of one-part geopolymers to be 650–700 °C (Sturm et al., 2016). Therefore, the binders in this study were also heated to 600 °C to test stability of lunar and Martian geopolymer binders at this threshold.

Accepted Manuscript
Version of record at: https://doi.org/10.1016/j.asr.2021.10.045

Other studies have tested specific simulants at higher temperatures to determine melt point and subsequent raw material properties for sintering, but that is not the objective of this study (Hintze and Quintana, 2013; Ray et al., 2010). Additionally, zeolitic materials may be formed rather than geopolymers when curing at temperatures in the range 90–200 °C which is not the intended outcome of this synthesis (Davidovits, 1991; Walton et al., 2001).

1.1. Geopolymer binders

Geopolymers are one type of alkali-activated alternate cementitious binder, produced by reacting amorphous aluminosilicate precursor powder with a highly concentrated aqueous alkali-hydroxide or alkali-silicate solution (Aupoil et al., 2019; Davidovits, 1991; Phair and Van Deventer, 2002; Zhang et al., 2013, 2012). The resulting material is a covalently bonded network. Geopolymer-type binders are of terrestrial interest given their capacity to reduce carbon emissions compared to ordinary Portland cement (OPC) (Peter Duxson et al., 2007c). Additionally, geopolymers can display higher compressive strength and greater temperature resistance compared with traditional cement (Alonso et al., 2017; Criado et al., 2009; Kong and Sanjayan, 2010). A broad range of aluminosilicate materials can be activated, from environmental clays and volcanic ash to industry waste, such as fly ash and slag. Much research on fly ash based geopolymers may be of use in developing lunar regolith geopolymers given their chemical similarity (Table 1). Fly ash geopolymers are typically cured at temperatures of 60–85 °C (Palomo et al., 1999) but have also been prepared under ambient conditions (Gao et al., 2015; Nath and Sarker, 2012, 2014), though lowering the temperature slows the reaction kinetics and lowers early strength (Puertas et al., 2000; Rovnaník, 2010; Sindhunata et al., 2006). The reader is directed to these reviews for further introduction to fly ash-based geopolymers (Duxson et al., 2007a; Khale and Chaudhary, 2007; Luukkonen et al., 2018; Provis, 2018; Shi et al., 2011; Singh and Middendorf, 2020; Zhang et al., 2020b).

The mechanical properties of concrete, including strength, fracture behavior, and workability, are affected by nanoscale material microstructure as well as chemical composition. Despite over a hundred of years of industrial production, the nano- and the micro-scale structure of cement paste is still a significant topic of research, especially as it relates to material processing (Moradian et al., 2019; Mostafa and Yahia, 2017; Reiter et al., 2018; Roussel et al., 2012; Zhang et al., 2020a). Much less is known about the nanoscale structure of geopolymers. The stoichiometry of geopolymers, generally represented as $M_n\{-(SiO_2)_q-AlO_2-\}_n$, is comprised of structural silica and alumina, and an alkali cation that balances the negative charge of tetravalent alumina, where n is degree of polycondensation, q is Si/Al ratio, and M is the alkali cation (Davidovits, 1991). Compositions with Si/Al stoichiometric ratios of 1, 2, or 3 and a Na/Al ratio of 1 are favored (Barbosa et al., 2000; Duxson et al., 2005b). A summary of many conditions in the form of a pseudo-ternary state diagram for sodium hydroxide activation has been proposed (Mills et al., 2022). Similar to advances in traditional cements, improvements in geopolymer cement and concrete properties can be anticipated through better understanding the microstructure and how it relates to the local mechanical properties (Chen et al., 2017; Duxson et al., 2005a; Duxson et al., 2007b; Fernández-Jiménez et al., 2006, 2005; Mills et al., 2021; Puligilla and Mondal, 2013; Rouyer and Poulesquen, 2015). Of particular interest is improved understanding and control of the kinetics of microstructure development and the associated impact on rheological property development. These relationships will be essential for additive manufacturing of geopolymer products and have been used to develop frameworks for additive manufacturing of OPC (Roussel, 2018).

1.2. Experimental objectives

The goal of this study was to create a framework to compare geopolymer binders from various lunar and Martian regolith simulants and under cure environments and

Table 1
Bulk chemistry analysis (wt%) of the simulants used in this study, also compared to a generic class F fly ash class composition. Trace elements (<0.5%) including NiO, SrO, Cr_2O_3 are omitted from this table but may be reported on the sources indicated.

Oxide	BP-1 (Stoeser et al., 2010)	JSC-1A (Hill et al., 2007)	LHS-1 (*Exolith*)	MGS-1 (*Exolith*)	MGS-1C (*Exolith*)	Fly ash, Class F (Typical) (Mindess et al., 2003)
SiO_2	47.2	46.2	48.1	45.2	44.8	>50
TiO_2	2.3	1.85	1.1	0.4	0.4	
Al_2O_3	16.7	17.1	25.8	14.9	9.8	20–30
FeO_T	12.1	11.2	3.7	18.7	12.0	<20
MgO	6.5	6.87	0.3	7.6	9.9	
CaO	9.2	9.43	18.4	10.0	15.3	<5
Na_2O	3.5	3.33				
K_2O	1.1	0.85	0.7	0.6	3.4	
MnO	0.21	0.19	0.1	0.1	0.1	
P_2O_5	0.52	0.62	1.0	0.9	1.0	
SO_3			0.3	0.9	2.3	
Cl			0.4	0.4	0.5	
Total	99.33	97.64	99.9	99.7	99.5	

Accepted Manuscript
Version of record at: https://doi.org/10.1016/j.asr.2021.10.045

exposures relevant to extra-terrestrial construction. The first objective was to successfully formulate geopolymer binders using the lunar regolith simulants BP-1, JSC-1A, and LHS-1 and Martian regolith simulants MGS-1 and MGS-1C. These simulants were specifically chosen based on their current use by NASA (BP-1 and JSC-1A), prevalence in previous literature studies (JSC-1A), importance to NASA ambitions (LHS-1, MGS-1), and likelihood of successful geopolymer binder formation (MGS-1C). The second objective was to measure material properties (compressive strength) and characterize microstructure of geopolymer binders after curing at ambient conditions (20 °C, 50% RH), low temperature (-80 °C), vacuum conditions and after exposure to extreme heat following ambient cure (600 °C). These results provide a context for the effect of variability in regolith composition, minerology, and particle morphology, as well as the effects of environmental conditions relevant to extra-terrestrial construction on geopolymer binder performance, useful for understanding results across the literature from unique regolith simulants. The results also illustrate differences between formulations based on lunar and Martian regolith simulants.

2. Materials and methods

2.1. Regolith simulants

The regolith simulants used in this work include three lunar simulants and two Martian simulants. Images of each of the simulants are shown in Fig. 1; chemical composition is given in Table 1. Two lunar simulants, BP-1 (Black Point) and JSC-1A (Johnson Space Center), were acquired courtesy of Kennedy Space Center's Swamp Works group, which leads excavation research with these specifically selected simulants. The third lunar simulant, LHS-1 (Lunar Highlands Simulant), was purchased from simulant developer Exolith Lab. Both BP-1 (Stoeser et al., 2010; Suescun-Florez et al., 2015) and JSC-1A (Alshibli and Hasan, 2009; Arslan et al., 2010; Hill et al., 2007; McKay et al., 1994; Ray et al., 2010; Sibille et al., 2006; Zeng et al., 2010) are sourced from the San Francisco Volcanic Field in northern Arizona, from the Black Point basalt flow and the Merriam crater, respectively. Note that BP-1 is effectively tailings of aggregate processing at an on-site quarry. JSC-1A is also sourced from a cinder quarry however it has undergone several milling operations. Both BP-1 and JSC-1A resemble low-titanium lunar mare terrain, though BP-1 is considered a geotechnical simulant for its lack of chemical similarity to Apollo mission samples (notably the higher proportion of TiO_2) (Stoeser et al., 2010), but the particle morphology is suggested to be more similar to lunar regolith (Rahmatian and Metzger, 2010). The LHS-1 simulant has not been sourced from any particular terrestrial source, rather it is developed to simulate the chemical composition and particle size distribution of lunar highlands soil brought back by the Apollo 16 mission. The highlands-type regolith is found in the lunar South Pole, which has been targeted for future landings of NASA's Artemis missions (Gawronska et al., 2020). Highlands regolith is relatively poorer in magnesium and iron compared to mare (Crawford, 2015), which is actually advantageous for geopolymer binder development.

Both Martian simulants, MGS-1 (Mars Global Simulant) and MGS-1C were also purchased from Exolith Lab. In contrast to lunar simulants, where Apollo mission samples serve as a basis of comparison, the development of

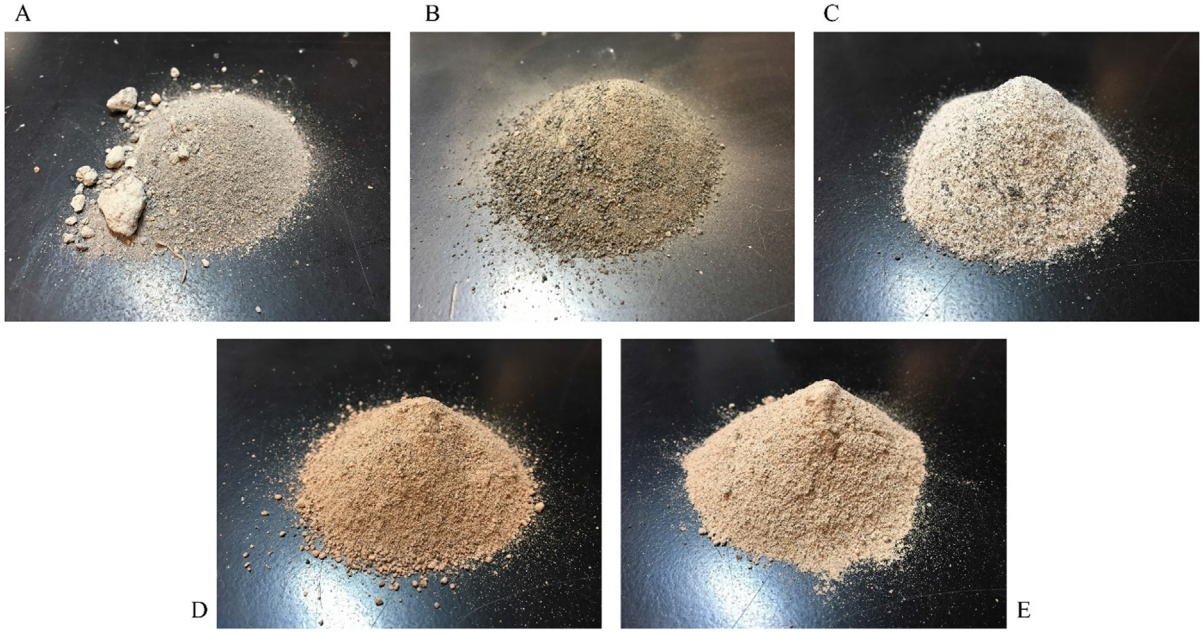

Fig. 1. Visual comparison of lunar and Martian simulants. (A) BP-1 Black Point lunar simulant; (B) JSC-1A Johnson Space Center lunar simulant; (C) LHS-1 Exolith Lab lunar highlands simulant; D) MGS-1 Exolith Lab Mars global simulant; (E) MGS-1C Exolith Lab Mars global simulant enriched with hydrated clay minerals (smectite).

Accepted Manuscript
Version of record at: https://doi.org/10.1016/j.asr.2021.10.045

Martian simulants relies on rover onboard instruments such as X-ray diffraction by the Curiosity rover. MGS-1 is particularly rich in iron oxide and was developed following mineral profiles according to Curiosity rover data; the chemical and mechanical properties of the simulant resemble the Rocknest windblown soil explored by Curiosity (Cannon et al., 2019). MGS-1C is a clay-enriched variant of MGS-1 (Cannon et al., 2017).

Previous studies have emphasized the need for reducing the particle size of the simulants to improve reactivity through milling (Alexiadis et al., 2017; Zhou et al., 2020), our own empirical observations confirmed that removing larger particles improved geopolymer conversion. In this study we chose to sieve the simulants using a No. 200 mesh size (75 μm) to reduce the energy requirement compared to milling and retain the original particle morphology. Scanning electron micrographs (SEMs) for each sieved simulant are shown in Fig. 2. Volume based particle size distributions measured by laser diffraction for each simulant after sieving are shown in Fig. 3 and corresponding distribution metrics are given in Table 2. It is noteworthy that the BP-1 simulant has a greater proportion of fine particles compared to the other lunar simulants, the d_{10} value is substantially smaller, which is particularly relevant given that a high specific surface area is important for alkali activation (Dietel et al., 2017; Rahier et al., 2003).

Most existing studies have been completed on JSC-1A (or similar simulants which are developed for chemical similarity to the Apollo missions), and thus this simulant may be regarded a *de facto* standard. But given the wide variability in both simulant type and properties explored in literature, in this research we seek to understand what effects variations in chemistry and particle size distribution between simulants may have on binder strength. Our variable simulants represent three main categories in which simulants may differ from JSC-1A: BP-1 is a geotechnical simulant with reduced mineralogical similarity, LHS-1 is a highlands simulant compared to a mare simulant (differing in TiO_2 content and minerology), and MGS-1 and MGS-1C are Martian simulants with notably higher iron and magnesium content than lunar simulants.

2.2. Methods

2.2.1. Simulant characterization

SEM: Scanning electron microscopy (SEM) was performed at the Keck Microscopy Institute at the University of Delaware using the Jeol JSM-7400F microscope.

Particle Size Distribution: A volume-based particle size distribution was measured using a Beckman Coulter LS 13 320 Particle Size Analyzer with dry powder module, after sieving regolith simulants with a #200 sieve to remove particles greater than 75 μm. For full context, Table 2 lists the particle size cutoffs for 10, 50, and 90% of the cumulative distribution of each simulant.

2.2.2. Formulation and curing

Binders were developed using the sieved regolith simulants and sodium silicate (37 wt%, Sigma Aldrich) at 71% regolith by weight for lunar simulants. Activation of MGS-1 was not possible using these conditions, but activation of MGS-1C was achieved after reducing the solids weight percent to 59%. Possible explanations for this observation are discussed in Section 3.1. The regolith simulant

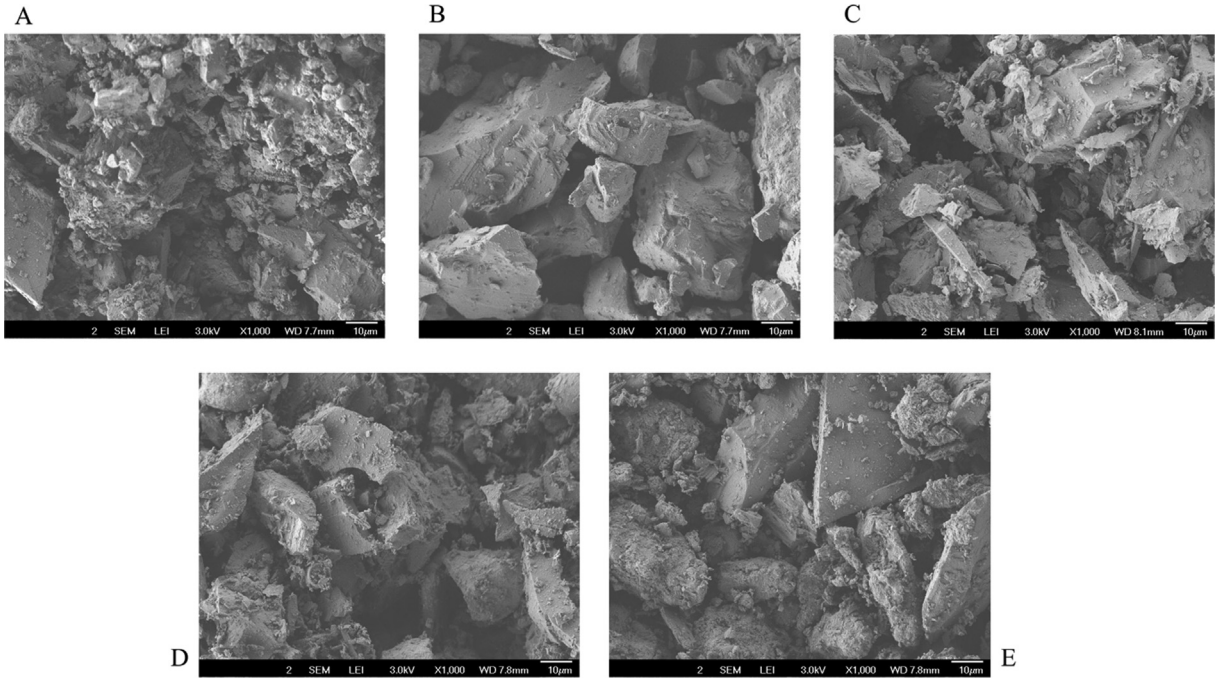

Fig. 2. Characteristic SEM images of lunar and Martian simulant particles < 75 μm, 1,000X magnification, white scale bar = 10 μm. (A) BP-1 Black Point lunar simulant; (B) JSC-1A Johnson Space Center lunar simulant; (C) LHS-1 Exolith Lab lunar highlands simulant; (D) MGS-1 Exolith Lab Mars global simulant; E) MGS-1C Exolith Lab Mars global simulant enriched with hydrated clay minerals (smectite).

Accepted Manuscript
Version of record at: https://doi.org/10.1016/j.asr.2021.10.045

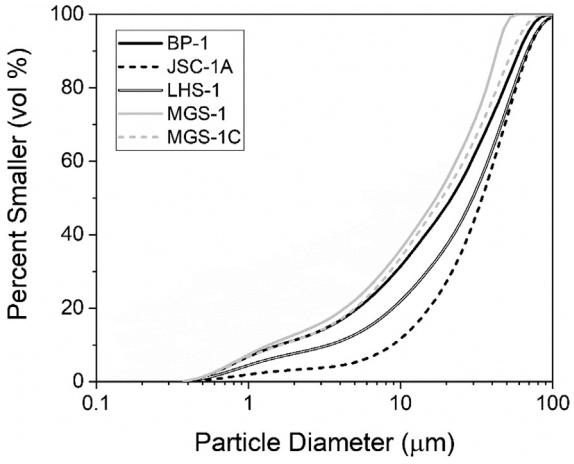

Fig. 3. Cumulative particle size distribution of simulants, measured as differential volume percent using laser particle size analysis after sieving regolith with sieve No. 200 (75 μm).

was added into the activator and mixed manually with a spatula for 5 min. The resulting mixture was cast into 0.5 in. cube molds (American Cube Mold Inc.) for a total of 24 cubes.

The cubes were cured for 7 days following one of four protocols designed to test for effects of high and low temperature and vacuum. The first subset of 6 cubes was cured in a laboratory oven at 20 °C and 50% RH for 7 days (ambient conditions). Another subset was cured at 20 °C and 50 %RH for 7 days, but on day 6 were subjected to one hour of heating at 600 °C in a Lindberg tube furnace. The temperature was monitored using a thermocouple and was consistent for the entire heating period. After heating, the cubes were allowed to cool to room temperature and then returned to ambient conditions until strength testing on day 7. The third subset of cubes was cured under vacuum at 20 °C for 7 days. The final subset of samples was cured for 4 days at ambient conditions, then cured for the remaining 3 days at −80 °C. Attempts to cure samples for 7 days at sub-zero temperatures were unsuccessful as the reaction kinetics are too slow under these conditions. Therefore, these samples represent low temperature 'exposure' rather than complete low temperature 'curing.'

2.2.3. Compressive strength testing

Compression tests were performed 7 day post-mixing for all samples. The cast cubes were weighed pre-compression and the dimensions of the loaded face were measured using calipers for calculation of compressive strength (CS). 7 day strength is not typically used for standard OPC evaluation, with only about 65% of strength formed at this time point. However, this is not the case for geopolymer cements; it has been documented that CS increases most rapidly in the initial 48 h or less (Davidovits, 1991; Hardjito et al., 2004b) and minimally between 1 and 2 weeks (Palomo et al., 2004). Therefore, it was deemed sufficient to test samples at 7 days.

Compression testing was performed using an Instron vertical loader retrofitted with MTS operating software. The load cell was an MTS model 661.19F-04, with a force capacity of 25 kN and cubes were compressed between two platens. The compression testing method is based on a modified ASTM C109 protocol, *Compression testing of hydraulic cement mortars* (Standard, 2008), where the cubes here are smaller due to limited resources and the cure time is reduced because geopolymers do not require 28 day to reach full strength. The rate of compression for these tests was 1 mm/min. The two cube faces normal to the platens were smoothed with sandpaper to remove irregularities and create a flat surface for compression. Care was also taken to center the samples along the axis of compression. The reported compressive strength (CS) σ is the average of the six measurements in each simulant subset, calculated using Equation (1), where F is the total maximum load and A is the area of the normal surface. Error bars represent the standard deviation of the 6 measurements.

$$\sigma = \frac{F}{A} \tag{1}$$

3. Results and discussion

3.1. Geopolymer binder properties

3.1.1. Comparison between simulants

Starting with the lunar geopolymer binders, the BP-1 geopolymer binder has the greatest compressive strength of the lunar simulants under ambient curing. From the SEM of the unreacted simulants (Fig. 5) there appears to be a greater proportion of small particles present on the surface of the grains than the other simulants. This is less obvious in the cumulative size distribution (Fig. 3) given the use of a volume based distribution which weights larger particles more greatly, but in Table 2 the d_{10} particle size of BP-1 is considerably less than JSC-1A and LHS-1, which could increase the inherent reactivity of BP-1 and lead to greater geopolymer conversion and resultant CS. Furthermore, JSC-1A has more larger particles than the other two lunar simulants, and the lowest CS under ambient and vacuum curing.

Additional factors may contribute to the low CS of JSC-1A binders under ambient and vacuum curing (Fig. 4). This simulant also has the lowest amorphous aluminosilicate content of the lunar simulants studied here (Fig. 6). It has been identified for fly ash geopolymers that not only the total aluminosilicate content but rather the 'reactive' aluminosilicate content is related to the ultimate material strength (Fernández-Jiménez et al., 2006). Therefore, in comparing the performance of the simulants, it is important to note not only the aluminosilicate content but the amorphous content as well (Fig. 6). Lunar soil contains both impact and volcanic glasses (McKay et al., 1991), and so amorphous vs glassy/crystalline aluminosilicate content should be considered when formulating lunar

Accepted Manuscript
Version of record at: https://doi.org/10.1016/j.asr.2021.10.045

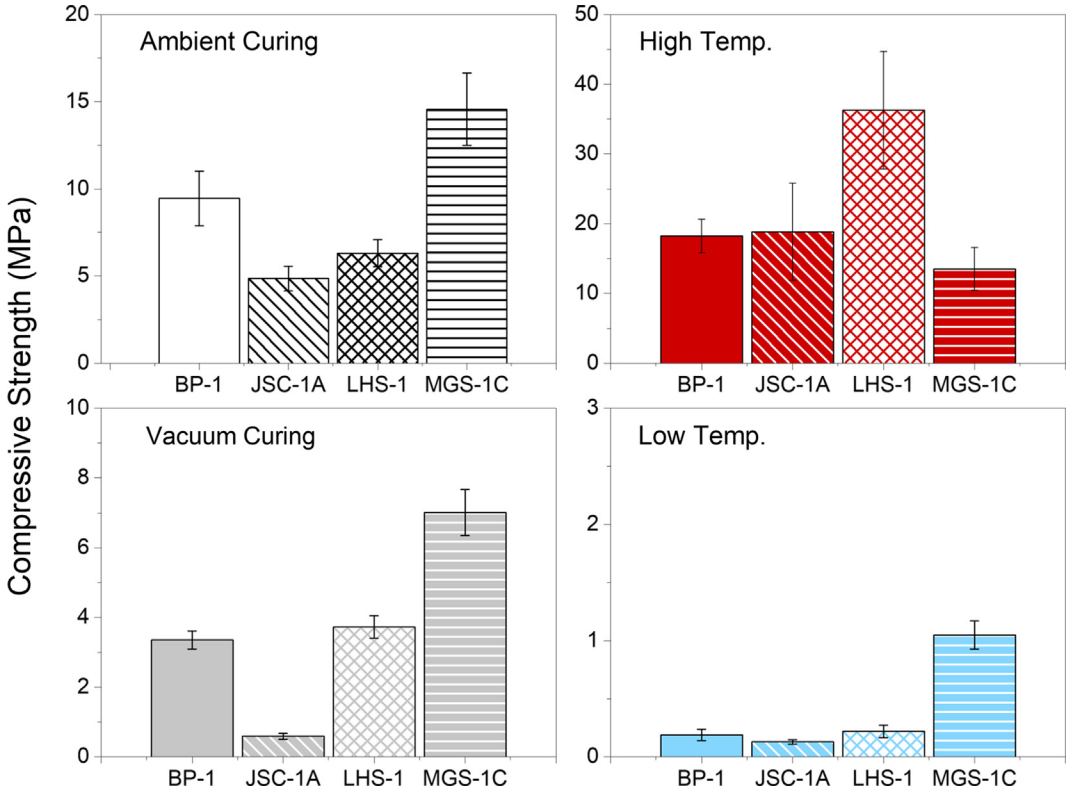

Fig. 4. Compressive strength (CS) of BP-1, JSC-1A, LHS-1, and MGS-1C geopolymer binders for each subset of environmental conditions: ambient curing, vacuum curing, high temperature exposure (1 h heating at 600 °C), and low temperature exposure (3 d cooling at −80 °C). CS represents average of six cubes, error bar represents standard deviation. No CS is available for MGS-1, which was not successfully activated in this study to produce a geopolymer binder. Note the change in vertical axis scaling for each subplot.

geopolymers. The greater amorphous aluminosilicate content could also explain the significantly higher CS of the LHS-1 binder after heating compared to the other lunar samples. The extreme temperature of 600 °C may effectively drive the geopolymer reaction to completion, converting all reactive (amorphous) aluminosilicate content into geopolymer product. Furthermore, the relatively low iron and magnesium content in LHS-1 could reduce the negative effect these elements have on the geopolymer binder at high temperatures, which will be discussed further with respect to the Martian binders.

The range of compressive strength (CS) in this study under ambient conditions is slightly lower than that of certain other geopolymer-type binders from lunar simulants cured under ambient conditions for 7 days reported in the literature (Davis et al., 2017; Zhou et al., 2020), but differences in the formulation of those binders are likely responsible, emphasizing again the importance for comparing binders from multiple simulants prepared under identical conditions in this study. The formulation and compressive strengths of the binders produced in this study compared to those reported in the literature are summarized in Tables A1 and A2 in the Appendix.

It is not practical to quantitatively compare the CS of the MGS-1C binder directly to the lunar geopolymer binders given the change in formulation necessary to achieve activation. The superior CS of the Martian MGS-1C binder (under conditions other than high temperature exposure) as compared to lunar binders studied here is attributed to the higher activator content in the former. Alexiadis et al. also observed the CS to increase in both lunar and Martian geopolymer binders when the concentration of activator was increased (Alexiadis et al., 2017). The increase in activator content in formulating Martian binders may therefore only positively affect the strength of the binder if sufficient aluminosilicate content is present for activation, as in the results for activating MGS-1C in this study as compared to MGS-1.

Comparing the reactivity of the two Martian simulants, the amorphous aluminosilicate content is more than double in MGS-1C compared to MGS-1, at the same time the relative content of iron- and magnesium-contributing minerals is greatly reduced (Fig. 6). The presence of magnesium sulfate in MSG-1 (4.0%) can hinder the activation of the simulant by sodium silicate due to the reactivity of the sulfate anion and sodium silicate (Bakharev, 2005; Yusuf, 2015); this component is reduced to 2.4% in the MGS-1C simulant. Fernandez-Jimenez and Palomo specifically observed that an Fe_2O_3 content<10% may be desired for optimizing mechanical strength in sodium-fly ash geopolymers, though this is an incidental finding and the lowered strength of samples with higher iron content may be also affected by the associated lowered reactive silica content (Fernández-Jiménez and Palomo, 2003). However, this finding is still impor-

Accepted Manuscript
Version of record at: https://doi.org/10.1016/j.asr.2021.10.045

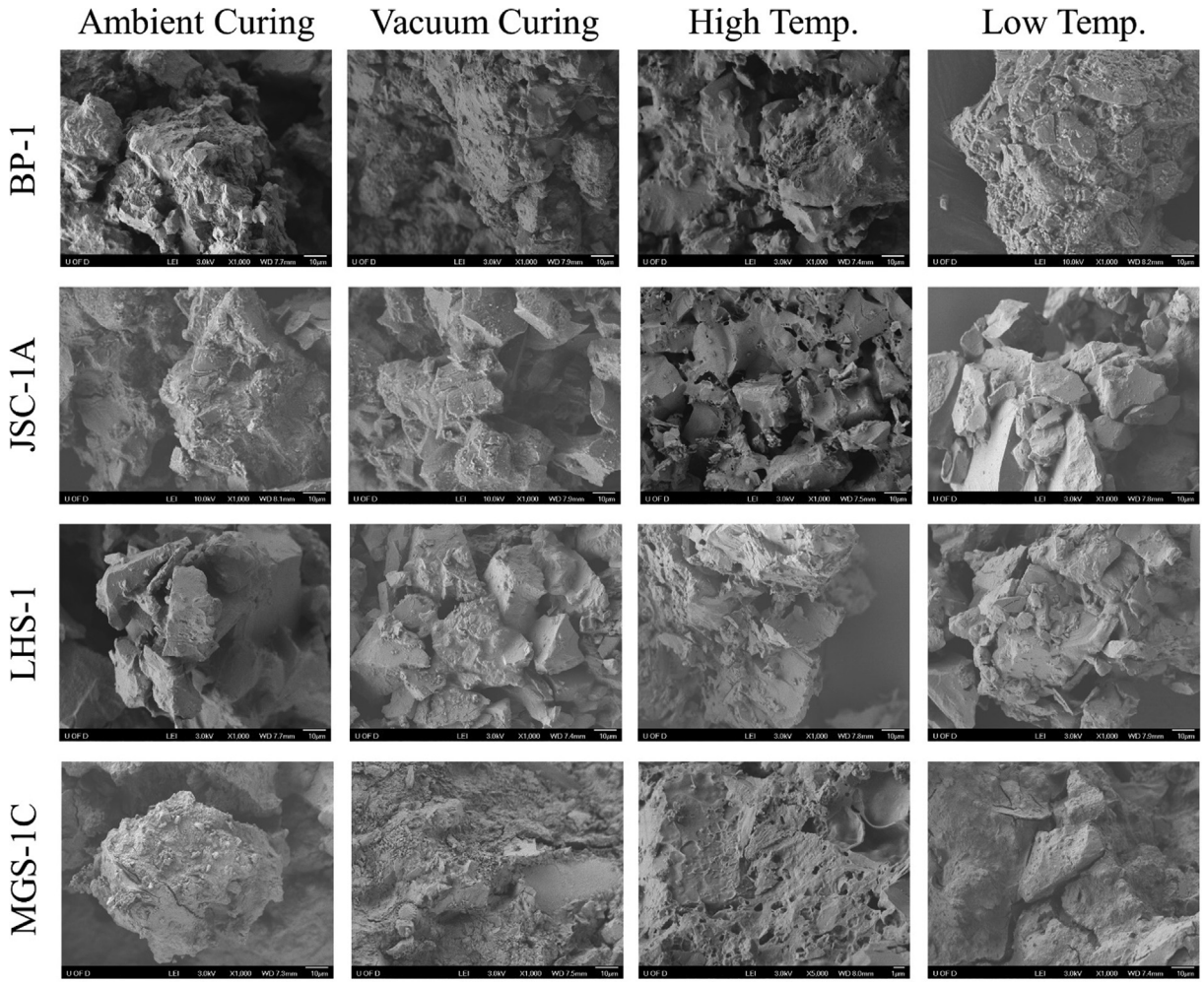

Fig. 5. Post-compression SEM images of the geopolymer binders, scale bar is 10 μm, 1000x magnification.

tant in the extension of developing geopolymers to Mars, where the iron oxide content is greater (Table 1) and therefore the reactive silica and alumina contents are lower than lunar counterparts.

Additionally, Rickard et al. (Rickard et al., 2011) noted that fly ash geopolymers (supplemented with both sodium silicate and sodium aluminate to control Si/Al) with increased iron content suffered much greater decrease in strength after exposure to high temperature (1000 °C) as compared to other samples with iron content<5%. The decrease in CS in the Martian binder in this study may be attributed to differences in coefficient of thermal expansion between iron oxides and the bulk geopolymer or crystallization of iron oxides (Rickard et al., 2011, 2010). These findings related to very high temperatures may be relevant to lunar application for VTVL pads where blast temperatures can reach up to 1200 °C on the launch pad ("Launch Pad 39B," 2020). The effect of iron content is more worrisome for the Martian environment, where iron content can be up to 10–20% compared to only 5–10% in lunar regolith (lowest in the LHS simulant). Also of note is that iron may participate in the geopolymer reaction, and in some cases may lead to increases in strength at less extreme temperatures (Kaze et al., 2017; Nongnuang et al., 2021).

3.1.2. Vacuum curing

Vacuum curing has an adverse effect on the 7 day CS of all geopolymer binders studied. Additionally, when demolding the samples, it appeared that some activating solution may have been expelled from the cubes onto the surrounding mold and then evaporated, based on the appearance of the mixes leaking out of the cubes, which was not observed in the molds cured at ambient conditions. The cubes were placed in the vacuum oven immediately after mixing, and therefore were not yet set, so any evaporation of solution would also inhibit the extent of reaction possible. A 'dry cast' formulation that requires pressure to activate the mix and uses less activating solution has been proposed, and this method resulted in comparable CS between samples cured under vacuum and ambient conditions (Davis et al., 2017). The context of both results implies that mixing and curing of geopolymer-type binders may require some pressurization on the lunar surface if a significant amount of activating solution is used. An energy

Accepted Manuscript
Version of record at: https://doi.org/10.1016/j.asr.2021.10.045

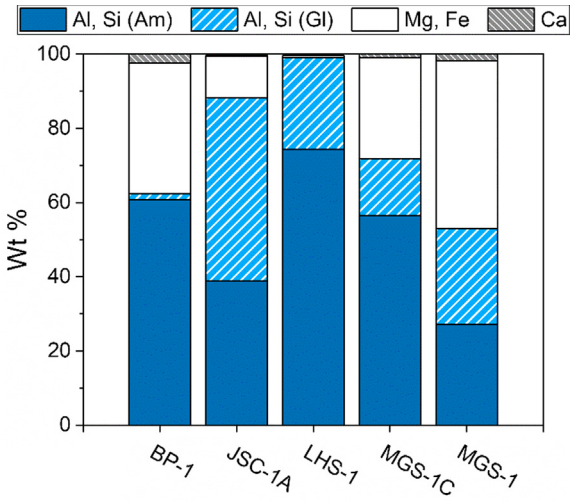

Fig. 6. Main mineral characterization of simulants – 1) amorphous aluminosilicate content (feldspar, smectite, plagioclase, labradorite, anorthosite) 2) glassy aluminosilicate content (glass-rich basalt [including plagioclase, pyroxene, olivine, and volcanic glass], quartz) 3) Minerals contributing magnesium and iron (olivine, augite, magnetite, hematite, ilmenite, pyroxene (bronzite), magnesium sulfide, iron carbonate, ferrihydrite, chrome spinel) 4) calcium-contributing minerals (anhydrite, calcite, apatite). Note that the anorthosite listed in LHS-1 and MGS-1 is comprised of both anorthite and albite, the former of which does contain calcium, but the breakdown between the two is not reported and is therefore included in the amorphous aluminosilicate category.

tradeoff analysis of the energy required for pressurizing binders from a dry-cast formulation vs providing an atmosphere for curing may be necessary to optimize the type of formulation used. Depending on the use of the binder, the CS of the vacuum cured lunar binders BP-1 and LHS-1 may be sufficient. The SEM micrographs of the vacuum cured samples show more similarity to the ambient cured and low temperature exposed samples than to the micrographs of the unreacted simulants, so while the geopolymer reaction may be hindered under these conditions it is not totally impeded and these samples are not merely cast simulant binders.

3.1.3. High temperature exposure

Exposure to high temperatures increased the strength of all lunar geopolymer binders compared to ambient curing. This result is attributed to the additional energy increasing the kinetics of the geopolymer reaction and forming further structure which contributes to the material strength. This result indicates that as expected for geopolymer binders, this range of temperature did not lead to material failure, as would be expected for OPC binders (Kong and Sanjayan, 2010). Future testing would be required to determine the expected surface temperature vs. time profile for a VTVL pad for ultimate thermal failure requirements.

A notable difference in the heated samples is the failure mechanism of the samples under compression: samples under ambient and vacuum curing and low temperature exposure typically failed via vertical compression and buckling along the axis orthogonal to compression but did not crumble into pieces. The heated samples did crack along the axis of compression, albeit at much higher loads than ambient samples (see Fig. 7). The difference in failure could be attributed to the microstructure where the heated samples display qualitatively more porosity than the other samples (Fig. 5), due to the structural water being expelled at high temperatures. The larger error bars seen in the heated samples may be due in part to this porosity and brittleness. Surface irregularities in heated samples resulting from thermal expansion also contribute to variability in testing of heated samples. This is especially apparent in the load vs displacement curves provided in the Appendix (Figs. A1 - A4), which also illustrate the difference in the energy dissipated by the samples due to the difference in failure mode. The energy is represented by the area under the load vs displacement curve ($E = F * A; [=]\mathrm{J}$). The heated samples have a greater increase in load over a smaller displacement which results in a lower energy dissipation despite the higher maximum load.

In contrast to the lunar binders, the Martian geopolymer binder MGS-1C displays a reduced CS after heating. There is also a change in the appearance of the samples from red-

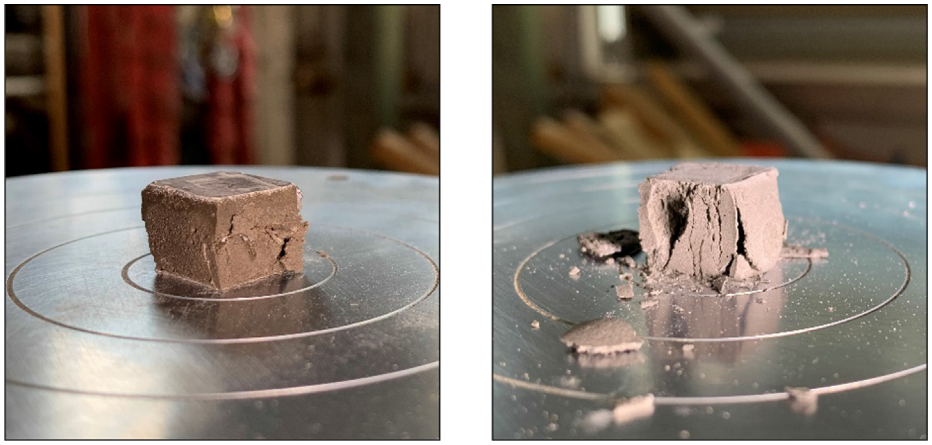

Fig. 7. Post-compression images of BP-1 binders showing differences in failure mechanisms, representative of all binders studied. **Left**: cube cured under ambient conditions, shows buckling in the center of the cube and compression. **Right**: cube exposed to high temperature, shows vertical cracking and shear failure.

Accepted Manuscript
Version of record at: https://doi.org/10.1016/j.asr.2021.10.045

dish brown pre-heating to grey post-heating. Both observations are attributed to the higher concentration of iron in the Martian simulants compared to the lunar simulants.

3.1.4. Low temperature exposure

Sub-zero temperatures also have an adverse effect on CS of all geopolymer binders studied (Fig. 4). Attempts to cure binders at −80 °C for the entirety of the 7 day period between mixing and compression were unsuccessful; to obtain data for exposure to this condition it was necessary to let the binders cure for an initial period of 4 days under ambient conditions. Despite this period of ambient curing the CS is significantly reduced for all samples. Future work to characterize the CS and structure of binders cured for 4 days under ambient conditions could elucidate whether the reaction is thermally quenched at 4 days and the CS of the samples exposed to low temperature reflect the 4 day extent of reaction, or whether there are additional effects related to the low temperature exposure. Given the different cycles of illumination on the moon and Mars, future studies of activation under conditions of thermal cycling are needed.

3.2. Feasibility estimations – VTVL pad construction

One critical application of lunar construction is VTVL pads to protect rockets from dust and debris on landing and takeoff (Gelino et al., 2021). An estimate of the feasibility of the methodology proposed here for use in lunar construction is made under the following assumptions. Terrestrial concrete columns require 400 kg of cement per m^3 of concrete structure (slab cement per concrete demand may be lower depending on strength requirements) (Mindess et al., 2003). For a geopolymer concrete consisting of lunar regolith (as cement substitute), aggregate, and an activating solution, the solid alkaline component is the only material needed to be launched from Earth. True lunar construction may require even less cement/concrete due to the lower strength demands resulting from the decrease in gravity, but this conservative estimate is used for approximations.

The Falcon Heavy payload capacity is currently 26,700 kg to geosynchronous orbit (GSO) and 16,800 kg to Mars (SpaceX, 2021). Kelso et al. used a 20 m pad in launch pad feasibility testing (Kelso et al., 2016) (Falcon Heavy is 12.2 m wide) and Ferguson et al. developed pavers for potential landing pad usage of 12 mm thickness (Ferguson et al., 2018). We also include estimates higher in material usage to illustrate a range of potential resource requirements, with a diameter of 50 m and thickness of 100 mm. Payload requirement for these hypothetical landing pads are listed in Table 3, assuming a geopolymer binder mix with 29% activator by weight, where the activator itself is 37% solids. These estimates range from 0.61% to 32% of GSO capacity, and 0.96% to 50% of Martian landing capacity, the lower ends of which (<1%) may be feasible. Note that it may be possible to partially source the necessary activation materials by taking advantage of weathering conditions existing on Mars (Burns, 1993; Ehlmann and Edwards, 2014; Hurowitz et al., 2006; White and Brantley, 2003) and other ISRU efforts.

Table 2
Particle size distribution analysis by laser diffraction of regolith simulants, where 10% of the distribution (by volume) has a particle size (diameter) less than the d_{10} particle size (etc. for d_{50}, d_{90}).

	Particle Size (μm)				
	BP-1	JSC-1	LHS-1	MGS-1C	MGS-1
d_{10}	1.76	9.73	3.74	1.78	1.48
d_{50}	23.8	37.8	32.7	20.5	18.8
d_{90}	66.5	76.2	74.8	59.8	47.25

Table 3
Alkali activator estimates for hypothetical circular VTVL pad construction.

Activator Requirement - Solids (kg)		
	d = 20 *m*	d = 50 *m*
h = 12 mm	1.62E + 02	1.01E + 03
h = 100 mm	1.35E + 03	8.43E + 03

4. Conclusions

Three lunar regolith simulants, representing both mare and highlands lunar regolith, and one Martian regolith simulant were successfully converted to geopolymer binders by alkali activation with sodium silicate. It was necessary to both increase the aluminosilicate content and decrease the solids content to activate the Martian simulant.

Amorphous aluminosilicate content and proportion of small particles are both thought to increase compressive strength (CS) of binders as they increase reactivity of the simulants. In each case of lunar simulant binder, the CS is increased after exposure to high temperature (600 °C) and reduced after exposure to low temperature (-80 °C) and vacuum. Iron and magnesium content, which are greater in the Martian simulants, are thought to lead to a reduction in CS after heating of Martian binders.

The results of the CS testing indicate that variability of chemical composition, minerology, and morphology of regolith simulants all impact the mechanical properties of the final binders. Comparing the strengths of binders formed in this study to others in the literature which differ in overall formulation and cure/processing conditions also emphasize the effect of those parameters on binder strength, which again underscores the need for understanding differences in simulant type to be able to compare results across studies with many variables.

Furthermore, this study reinforces the observation that reaction kinetics are closely linked to chemical composition, and therefore extreme environments such as high and low temperature and low pressure can compound the effect of chemical differences on reaction extent and geopolymer binder conversion and lead to more variability in CS between simulants.

These experiments demonstrate the possibility of creating geopolymer binders with sufficient CS using lunar and Martian regolith simulant within current payload con-

Accepted Manuscript
Version of record at: https://doi.org/10.1016/j.asr.2021.10.045

straints; however, optimization of final mix design and scale up to concrete mixes that include aggregate will be required before implementation. The results of this study support the need for further development of geopolymer-type binders for extra-terrestrial ISRU construction. Additionally, this study provides a framework for understanding what differences may exist between regolith simulants, given the variability in this research worldwide. Furthermore, the environmental conditions studied represent a limited exposure of the binders to conditions that may be experienced by lunar and Martian cements. Further research studying the effects of thermal cycling, the combined effects of vacuum and temperature, and exposure to true rocket engine will be necessary before implementation is possible.

Declaration of Competing Interest

The authors declare that they have no known competing financial interests or personal relationships that could have appeared to influence the work reported in this paper.

Acknowledgements

The authors acknowledge the financial support provided by the National Aeronautics and Space Administration (NASA EPSCoR Grants 80NSSC19M0017 and 80NSSC19M0087). Additional funding support was provided by Delaware Space Grant College and Fellowship Program (NASA Grant 80NSSC20M0045). This work was completed in part with equipment resources provided by the University of Delaware Structural and Geotechnical Lab courtesy of Gary Wenczel and the University of Delaware Energy Conversion Institute courtesy of Prof. William Shafarman. The authors thank Kevin M. Cannon, Robert P. Mueller, and Warren P. Ruemmele for insightful discussions.

Appendix.

Table A1
Summary of geopolymer formulation and compressive strength (CS) from this study. CS represents the average of six samples in all cases except JSC-1A, vacuum (5), LHS-1 low temp. (5), where one sample in each case was deformed upon demolding and could not be tested. Replicate batches of select cases were also produced to verify reproducibility. Activator is sodium silicate (SS).

Simulant	Simulant Type	Activator	Wt% Solids	7d Compressive Strength (MPa)			
				Ambient Curing (20 °C)	Vacuum Curing (20 °C, 0 inHg)	Ambient Curing, 1 h Heating 600 °C	4d Ambient Curing, 3d Cooling −80 °C
BP-1	Lunar mare, Geotechnical	SS	71	9.44	3.35	18.22	0.19
JSC-1A	Lunar mare, Apollo 14-based	SS	71	4.86	0.59	18.81	0.18
LHS-1	Lunar highlands, Apollo 16- based	SS	71	6.31	3.73	36.25	0.22
MGS-1C	Martian, clay enriched	SS	59	13.59	7.47	12.16	1.47

Table A2
Comparison of formulations and compressive strength (CS) reported for lunar and Martian geopolymer binders in the literature. CS for Alexiadis, Davis, and Montes samples is reported from tabulated values, CS for Pilehvar and Zhou samples is estimated from plots. Sodium silicate activator is abbreviated as SS.

Source	Simulant	Simulant Type	Activator	Wt% Solids	Curing	Compressive Strength MPa
(Alexiadis et al., 2017)	JSC-1A L	Lunar mare, Apollo-based	2 M NaOH		3 h at 80 °C,	2 (28d)
	JSC-1A L	Lunar mare, Apollo-based	4 M NaOH		28 d at RT	3.7 (28d)
	JSC-1A L	Lunar mare, Apollo-based	6 M NaOH			7.8 (28d)
	JSC-1A L	Lunar mare, Apollo-based	8 M NaOH			18.4 (28d)
	JSC-1A M	Martian	2 M NaOH			1.4 (28d)
	JSC-1A M	Martian	4 M NaOH			1 (28d)
	JSC-1A M	Martian	6 M NaOH			0.7 (28d)
	JSC-1A M	Martian	8 M NaOH			2.5 (28d)
(Pilehvar et al., 2020)	DNA-1	Lunar mare, Apollo/JSC-1A-based	NaOH	74	6 h at 80 °C, followed by freeze–thaw cycles at −80/80 °C held for 48 h	16 (0 cycles), 25 (1 cycle), 23 (2 cycles), 33 (3 cycles)
(Davis et al., 2017)	JSC-1A	Lunar mare, Apollo 14-based	NaOH/SS	94, dry cast (pressurized at 14 MPa)	26 °C	10.71 (7d)
					26 °C, vacuum	11.35 (7d), 9.26 (28d)
					106 °C	11.63 (7d), 15.34 (28d)
					106 °C, vacuum	7.91 (7d)
(Montes et al., 2015)	JSC-1A	Lunar mare, Apollo 14-based	NaOH/SS	76	72 h at 60 °C	16.62 (3d)
				83 (dry cast)	7d at 23 °C	33.07 (7d)
				83 (dry cast)	72 h at 60 °C	37.63 (3d)
(Zhou et al., 2020)	BH-1	Lunar mare, Apollo 16-based	NaOH/SS	81	20 °C	15 (7d), 21 (28d)

Accepted Manuscript
Version of record at: https://doi.org/10.1016/j.asr.2021.10.045

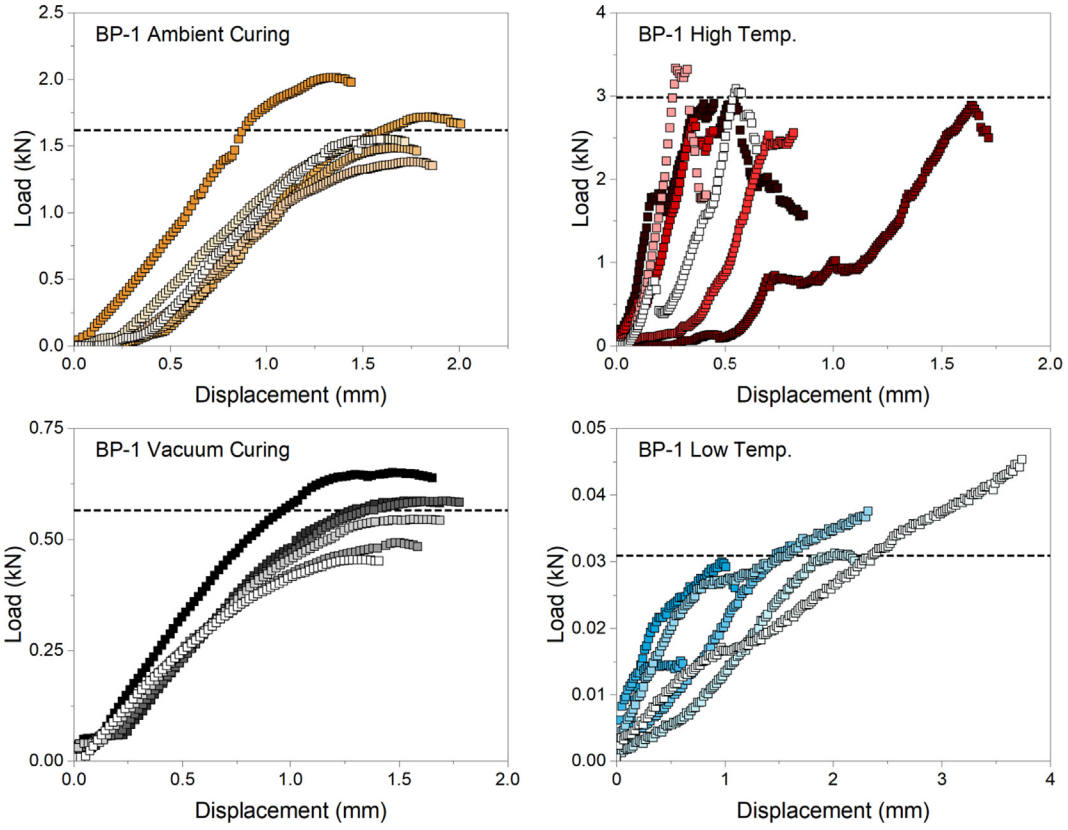

Fig. A1. Load vs displacement curves of BP-1 geopolymer binders under ambient and vacuum curing and high and low temperature exposure. Dashed line indicates average maximum load.

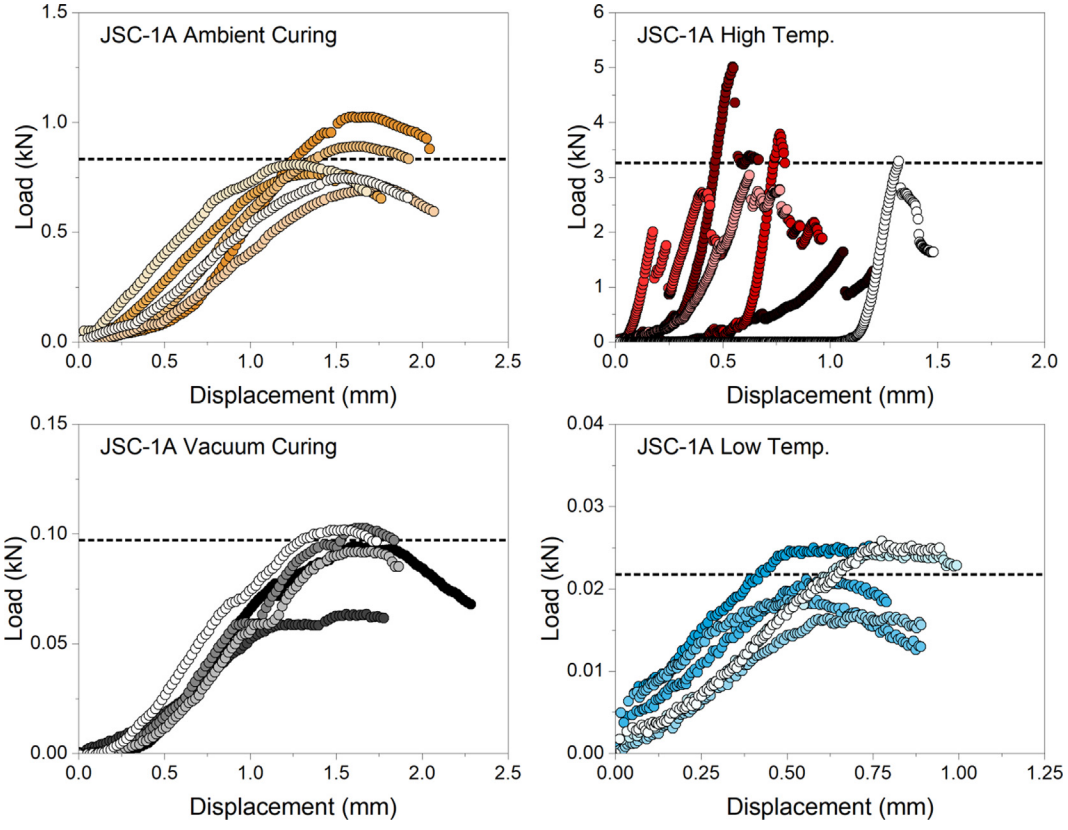

Fig. A2. Load vs displacement curves of JSC-1A geopolymer binders under ambient and vacuum curing and high and low temperature exposure. Dashed line indicates average maximum load.

Accepted Manuscript
Version of record at: https://doi.org/10.1016/j.asr.2021.10.045

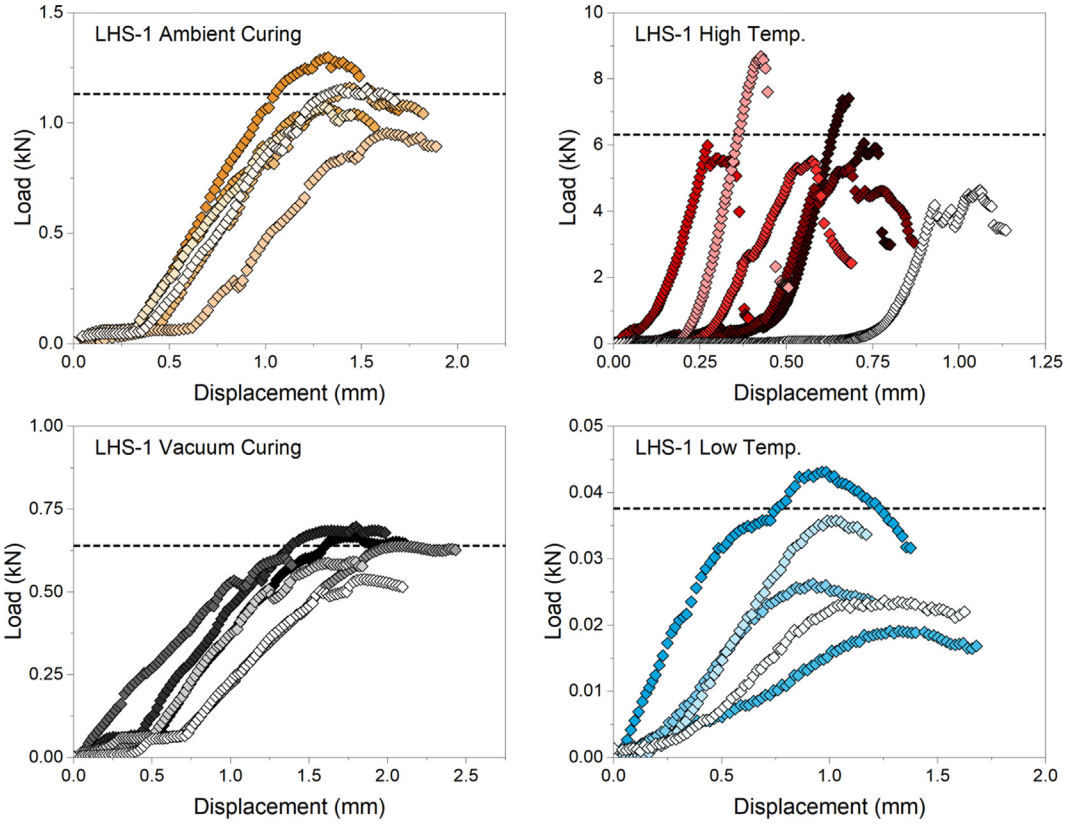

Fig. A3. Load vs displacement curves of LHS-1 geopolymer binders under ambient and vacuum curing and high and low temperature exposure. Dashed line indicates average maximum load.

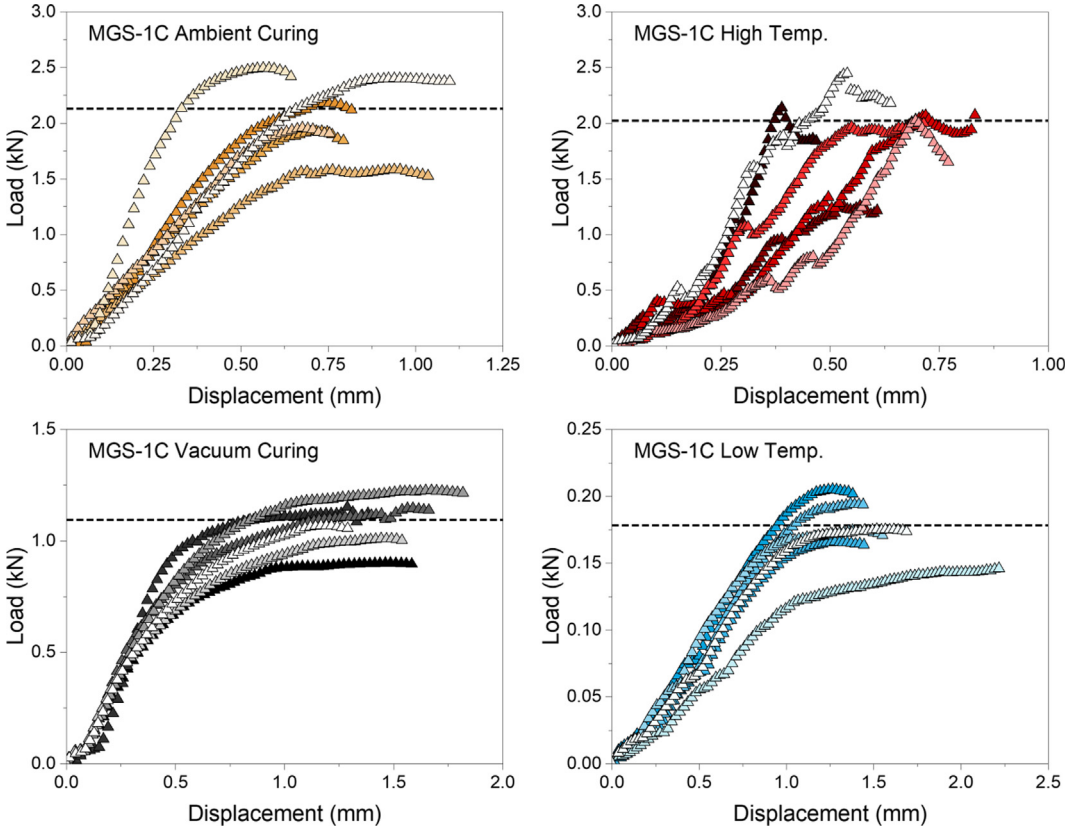

Fig. A4. Load vs displacement curves of MGS-1C geopolymer binders under ambient and vacuum curing and high and low temperature exposure. Dashed line indicates average maximum load.

References

Alexiadis, A., Alberini, F., Meyer, M.E., 2017. Geopolymers from lunar and Martian soil simulants. Adv. Sp. Res. 59, 490–495. https://doi.org/10.1016/j.asr.2016.10.003.

Allen, C.C., Morris, R.V., Jager, K.M., Golden, D.C., Lindstrom, D.J., Lindstrom, M., Lockwood, J.P., 1998. Martian Regolith Simulant JSC Mars-1. In: Lunar and Planetary Science XXIX. Houston, TX, pp. 1690–1691.

Alonso, M.M., Gismera, S., Blanco, M.T., Lanzón, M., Puertas, F., 2017. Alkali-activated mortars: Workability and rheological behaviour. Constr. Build. Mater. 145, 576–587. https://doi.org/10.1016/j.conbuildmat.2017.04.020.

Alshibli, K.A., Hasan, A., 2009. Strength Properties of JSC-1A Lunar Regolith Simulant. J. Geotech. Geoenvironmental Eng. 135, 673–679. https://doi.org/10.1061/(asce)gt.1943-5606.0000068.

Anand, M., Crawford, I.A., Balat-Pichelin, M., Abanades, S., Van Westrenen, W., Péraudeau, G., Jaumann, R., Seboldt, W., 2012. A brief review of chemical and mineralogical resources on the Moon and likely initial in situ resource utilization (ISRU) applications. Planet. Space Sci. 74, 42–48. https://doi.org/10.1016/j.pss.2012.08.012.

Arslan, H., Batiste, S., Sture, S., 2010. Geotechnical engineering properties of lunar soil simulants. Lunar Settlements 23, 637–647. https://doi.org/10.1201/9781420083330.

ASTM C109 / C109M-21, Standard Test Method for Compressive Strength of Hydraulic Cement Mortars (Using 2-in. or [50 mm] Cube Specimens), ASTM International, West Conshohocken, PA, 2021, www.astm.org.

Aupoil, J., Champenois, J.B., d'Espinose de Lacaillerie, J.B., Poulesquen, A., 2019. Interplay between silicate and hydroxide ions during geopolymerization. Cem. Concr. Res. 115, 426–432. https://doi.org/10.1016/j.cemconres.2018.09.012.

Bakharev, T., 2005. Durability of geopolymer materials in sodium and magnesium sulfate solutions. Cem. Concr. Res. 35, 1233–1246. https://doi.org/10.1016/j.cemconres.2004.09.002.

Barbosa, V.F.F., MacKenzie, K.J.D., Thaumaturgo, C., 2000. Synthesis and characterisation of materials based on inorganic polymers of alumina and silica: Sodium polysialate polymers. Int. J. Inorg. Mater. 2, 309–317. https://doi.org/10.1016/S1466-6049(00)00041-6.

Buchner, C., Pawelke, R.H., Schlauf, T., Reissner, A., Makaya, A., 2018. A new planetary structure fabrication process using phosphoric acid. Acta Astronaut. 143, 272–284. https://doi.org/10.1016/j.actaastro.2017.11.045.

Burns, R.G., 1993. Rates and mechanisms of chemical weathering of ferromagnesian silicate minerals on Mars. Geochim. Cosmochim. Acta 57, 4555–4574. https://doi.org/10.1016/0016-7037(93)90182-V.

Cannon, K.M., Britt, D.T., Smith, T.M., Fritsche, R.F., Batcheldor, D., 2019. Mars global simulant MGS-1: A Rocknest-based open standard for basaltic martian regolith simulants. Icarus 317, 470–478. https://doi.org/10.1016/j.icarus.2018.08.019.

Cannon, K.M., Parman, S.W., Mustard, J.F., 2017. Primordial clays on Mars formed beneath a steam or supercritical atmosphere. Nature 552, 88–91. https://doi.org/10.1038/nature24657.

Cesaretti, G., Dini, E., De Kestelier, X., Colla, V., Pambaguian, L., 2014. Building components for an outpost on the Lunar soil by means of a novel 3D printing technology. Acta Astronaut. 93, 430–450. https://doi.org/10.1016/j.actaastro.2013.07.034.

Chen, X., Sutrisno, A., Zhu, L., Struble, L.J., 2017. Setting and nanostructural evolution of metakaolin geopolymer. J. Am. Ceram. Soc. 100, 2285–2295. https://doi.org/10.1111/jace.14641.

Crawford, I.A., 2015. Lunar resources: A review. Prog. Phys. Geogr. 39, 137–167. https://doi.org/10.1177/0309133314567585.

Criado, M., Palomo, A., Fernández-Jiménez, A., Banfill, P.F.G., 2009. Alkali activated fly ash: Effect of admixtures on paste rheology. Rheol. Acta 48, 447–455. https://doi.org/10.1007/s00397-008-0345-5.

Davidovits, J., 1991. Geopolymers. J. Therm. Anal. 37, 1633–1656. https://doi.org/10.1007/BF01912193.

Davis, G., Montes, C., Eklund, S., 2017. Preparation of lunar regolith based geopolymer cement under heat and vacuum. Adv. Sp. Res. 59, 1872–1885. https://doi.org/10.1016/j.asr.2017.01.024.

Dietel, J., Warr, L.N., Bertmer, M., Steudel, A., Grathoff, G.H., Emmerich, K., 2017. The importance of specific surface area in the geopolymerization of heated illitic clay. Appl. Clay Sci. 139, 99–107. https://doi.org/10.1016/j.clay.2017.01.001.

Duxson, P., Fernández-Jiménez, A., Provis, J.L., Lukey, G.C., Palomo, A., Van Deventer, J.S.J., 2007a. Geopolymer technology: The current state of the art. J. Mater. Sci. 42, 2917–2933. https://doi.org/10.1007/s10853-006-0637-z.

Duxson, P., Mallicoat, S.W., Lukey, G.C., Kriven, W.M., van Deventer, J.S.J., 2007b. The effect of alkali and Si/Al ratio on the development of mechanical properties of metakaolin-based geopolymers. Colloids Surfaces A Physicochem. Eng. Asp. 292, 8–20. https://doi.org/10.1016/j.colsurfa.2006.05.044.

Duxson, P., Provis, J.L., Lukey, G.C., Mallicoat, S.W., Kriven, W.M., Van Deventer, J.S.J., 2005a. Understanding the relationship between geopolymer composition, microstructure and mechanical properties. Colloids Surfaces A Physicochem. Eng. Asp. 269, 47–58. https://doi.org/10.1016/j.colsurfa.2005.06.060.

Duxson, P., Provis, J.L., Lukey, G.C., Separovic, F., Van Deventer, J.S.J., 2005b. 29Si NMR study of structural ordering in aluminosilicate geopolymer gels. Langmuir 21, 3028–3036. https://doi.org/10.1021/la047336x.

Duxson, P., Provis, J.L., Lukey, G.C., van Deventer, J.S.J., 2007c. The role of inorganic polymer technology in the development of "green concrete". Cem. Concr. Res. 37, 1590–1597. https://doi.org/10.1016/j.cemconres.2007.08.018.

Ehlmann, B.L., Edwards, C.S., 2014. Mineralogy of the Martian surface. Annu. Rev. Earth Planet. Sci. 42, 291–315. https://doi.org/10.1146/annurev-earth-060313-055024.

Fateri, M., Meurisse, A., Sperl, M., Urbina, D., Madakashira, H.K., Govindaraj, S., Gancet, J., Imhof, B., Hoheneder, W., Waclavicek, R., Preisinger, C., Podreka, E., Mohamed, M.P., Weiss, P., 2019. Solar Sintering for Lunar Additive Manufacturing. J. Aerosp. Eng. 32, 04019101. https://doi.org/10.1061/(asce)as.1943-5525.0001093.

Ferguson, R.E., Shafirovich, E., Mantovani, J.G., 2018. Combustion Joining of Regolith Tiles for In Situ Fabrication of Launch/Landing Pads on the Moon and Mars. In: Earth and Space 2018. American Society of Civil Engineers, Reston, VA, pp. 281–288. https://doi.org/10.1061/9780784481899.028.

Fernández-Jiménez, A., Palomo, A., 2003. Characterisation of fly ashes. Potential reactivity as alkaline cements. Fuel 82, 2259–2265. https://doi.org/10.1016/S0016-2361(03)00194-7.

Fernández-Jiménez, A., Palomo, A., Criado, M., 2005. Microstructure development of alkali-activated fly ash cement: A descriptive model. Cem. Concr. Res. 35, 1204–1209. https://doi.org/10.1016/j.cemconres.2004.08.021.

Fernández-Jiménez, A., Palomo, A., Sobrados, I., Sanz, J., 2006. The role played by the reactive alumina content in the alkaline activation of fly ashes. Microporous Mesoporous Mater. 91, 111–119. https://doi.org/10.1016/j.micromeso.2005.11.015.

Gao, X., Yu, Q.L., Brouwers, H.J.H., 2015. Reaction kinetics, gel character and strength of ambient temperature cured alkali activated slag-fly ash blends. Constr. Build. Mater. 80, 105–115. https://doi.org/10.1016/j.conbuildmat.2015.01.065.

Gawronska, A.J., Barrett, N., Boazman, S.J., Gilmour, C.M., Halim, S. H., Harish, McCanaan, K., Satyakumar, A. V., Shah, J., Meyer, H. M., Kring, D.A., 2020. Geologic context and potential EVA targets at the lunar south pole. Adv. Sp. Res. 66, 1247–1264. https://doi.org/10.1016/j.asr.2020.05.035

Gelino, N.J., Mueller, R.P., Moses, R.W., Mantovani, J.G., Metzger, P. T., Buckles, B.C., Sibille, L., 2021. Off Earth Landing and Launch Pad Construction—A Critical Technology for Establishing a Long-Term Presence on Extraterrestrial Surfaces. In: Earth and Space 2021. American Society of Civil Engineers, Reston, VA, pp. 855–869. https://doi.org/10.1061/9780784483374.079.

.

Happel, J.A., 1993. Indigenous materials for lunar construction. Appl. Mech. Rev. 46, 313–325. https://doi.org/10.1115/1.3120360.

Hardjito, D., Wallah, S.E., Sumajouw, D.M.J., Rangan, B.V., 2004a. Factors influencing the compressive strength of fly ash-based geopolymer concrete. Civ. Eng. Dimens. 6, 88–93. https://doi.org/10.9744/ced.6.2. pp. %2088-93.

Hardjito, Djwantoro, Wallah, S.E., Sumajouw, D.M.J., Rangan, B.V., 2004. On the development of fly ash-based geopolymer concrete. ACI Mater. J. 101, 467–472. https://doi.org/10.14359/13485

Haskin, L., Warren, P., 1991. Lunar chemistry, in: Grant H. Heiken, David T. Vaniman, B.M.F. (Ed.), Lunar Sourcebook: A User's Guide to the Moon. Cambridge University Press, pp. 357–474.

Hill, E., Mellin, M.J., Deane, B., Liu, Y., Taylor, L.A., 2007. Apollo sample 70051 and high- and low-Ti lunar soil simulants MLS-1A and JSC-1A: Implications for future lunar exploration. J. Geophys. Res. E Planets 112, 1–11. https://doi.org/10.1029/2006JE002767.

Hintze, P.E., Quintana, S., 2013. Building a Lunar or Martian Launch Pad with In Situ Materials: Recent Laboratory and Field Studies. J. Aerosp. Eng. 26, 134–142. https://doi.org/10.1061/(asce)as.1943-5525.0000205.

Hurowitz, J.A., McLennan, S.M., Tosca, N.J., Arvidson, R.E., Michalski, J.R., Ming, D.W., Schröder, C., Squyres, S.W., 2006. In situ and experimental evidence for acidic weathering of rocks and soils on Mars. J. Geophys. Res. E Planets 111, 1–16. https://doi.org/10.1029/2005JE002515.

Imhof, B., Urbina, D., Weiss, P., Sperl, M., 2017. Advancing Solar Sintering for Building A Base On The Moon Barbara Imhof. In: 69th International Astronautical Congress (IAC), Adelaide, Australia, 25–29 September 2017. International Astronautical Federation, Adelaide, Australia, pp. 1–17.

Kaze, R.C., Beleuk à Moungam, L.M., Fonkwe Djouka, M.L., Nana, A., Kamseu, E., Chinje Melo, U.F., Leonelli, C., 2017. The corrosion of kaolinite by iron minerals and the effects on geopolymerization. Appl. Clay Sci. 138, 48–62. https://doi.org/10.1016/j.clay.2016.12.040

Kelso, R.M., Romo, R., Andersen, C., Mueller, R.P., Lippitt, T., Gelino, N.J., Smith, J.D., Townsend, I.I., Schuler, J.M., Nugent, M.W., Nick, A.J., Zacny, K., Hedlund, M., 2016. Exploration and Utilization of Extra-Terrestrial Bodies. In: Earth and Space 2016. American Society of Civil Engineers, Reston, VA, pp. 653–667. https://doi.org/10.1061/9780784479971.061.

Khale, D., Chaudhary, R., 2007. Mechanism of geopolymerization and factors influencing its development: A review. J. Mater. Sci. 42, 729–746. https://doi.org/10.1007/s10853-006-0401-4.

Khoshnevis, B., Bodiford, M.P., Burks, K.H., Ethridge, E., Tucker, D., Kim, W., Toutanji, H., Fiske, M.R., 2005. Lunar contour crafting - A novel technique for ISRU-based habitat development. 43rd AIAA Aerosp. Sci. Meet. Exhib. - Meet. Pap, 7397–7409. https://doi.org/10.2514/6.2005-538.

Khoshnevis, B., Yuan, X., Zahiri, B., Zhang, J., Xia, B., 2016. Construction by Contour Crafting using sulfur concrete with planetary applications. Rapid Prototyp. J. 22, 848–856. https://doi.org/10.1108/RPJ-11-2015-0165.

King, P.L., McLennan, S.M., 2010. Sulfur on mars. Elements 6, 107–112. https://doi.org/10.2113/gselements.6.2.107.

Kong, D.L.Y., Sanjayan, J.G., 2010. Effect of elevated temperatures on geopolymer paste, mortar and concrete. Cem. Concr. Res. 40, 334–339. https://doi.org/10.1016/j.cemconres.2009.10.017.

Launch Pad 39B [WWW Document], 2020. NASA. URL https://www.nasa.gov/content/launch-pad-39b

Lepper, K., McKeever, S.W.S., 2000. Characterization of fundamental luminescence properties of the mars soil simulant JSC Mars-1 and their relevance to absolute dating of martian eolian sediments. Icarus 144, 295–301. https://doi.org/10.1006/icar.1999.6295.

Li, S., Lucey, P.G., Milliken, R.E., Hayne, P.O., Fisher, E., Williams, J.P., Hurley, D.M., Elphic, R.C., 2018. Direct evidence of surface exposed water ice in the lunar polar regions. Proc. Natl. Acad. Sci. U. S. A. 115, 8907–8912. https://doi.org/10.1073/pnas.1802345115.

Lin, T.D., Love, H., Stark, D., 1992. Physical Properties of Concrete Made with Apollo 16 Lunar Soil Sample, in: The Second Conference on Lunar Bases and Space Activities of the 21st Century. NASA, Johnson Space Center, pp. 483-4872–533. https://doi.org/10.2514/5.9781600865855.0522.0533

Luukkonen, T., Abdollahnejad, Z., Yliniemi, J., Kinnunen, P., Illikainen, M., 2018. One-part alkali-activated materials: A review. Cem. Concr. Res. 103, 21–34. https://doi.org/10.1016/j.cemconres.2017.10.001.

McKay, D.S., Carter, J.L., Boles, W.W., Allen, C.C., Allton, H.H., 1994. New lunar soil simulant. Proc. 4th Int. Conf. Eng. Constr. Oper. Sp, 857–866.

McKay, D.S., Heiken, G., Basu, A., Blanford, G., Simon, S., Reedy, R., French, B.M., Papike, J., 1991. The Lunar Regolith, in: Grant H. Heiken, David T. Vaniman, B.M.F. (Ed.), Lunar Sourcebook. Cambridge University Press, pp. 285–356.

Meurisse, A., Makaya, A., Willsch, C., Sperl, M., 2018. Solar 3D printing of lunar regolith. Acta Astronaut. 152, 800–810. https://doi.org/10.1016/j.actaastro.2018.06.063.

Mills, J.N., Mondal, P., Wagner, N.J., 2022. Structure-property relationships and state behavior of alkali-activated aluminosilicate gels. Cem. Concr. Res. 151. https://doi.org/10.1016/j.cemconres.2021.106618 106618.

Mills, J.N., Wagner, N.J., Mondal, P., 2021. Relating chemical composition, structure, and rheology in alkali-activated aluminosilicate gels. J. Am. Ceram. Soc. 104, 572–583. https://doi.org/10.1111/jace.17459.

Mindess, S., Darwin, D., Young, J.F., 2003. Concrete, 2nd Edition. Tech, Doc.

Montes, C., Broussard, K., Gongre, M., Simicevic, N., Mejia, J., Tham, J., Allouche, E., Davis, G., 2015. Evaluation of lunar regolith geopolymer binder as a radioactive shielding material for space exploration applications. Adv. Sp. Res. 56, 1212–1221. https://doi.org/10.1016/j.asr.2015.05.044.

Moradian, M., Hu, Q., Aboustait, M., Ley, M.T., Hanan, J.C., Xiao, X., Rose, V., Winarski, R., Scherer, G.W., 2019. Multi-scale observations of structure and chemical composition changes of portland cement systems during hydration. Constr. Build. Mater. 212, 486–499. https://doi.org/10.1016/j.conbuildmat.2019.04.013.

Moraes Neves, J., Collins, P.J., Wilkerson, R.P., Grugel, R.N., Radlińska, A., 2019. Microgravity Effect on Microstructural Development of Tricalcium Silicate (C3S) Paste. Front. Mater. 6, 1–12. https://doi.org/10.3389/fmats.2019.00083.

Mostafa, A.M., Yahia, A., 2017. Physico-chemical kinetics of structural build-up of neat cement-based suspensions. Cem. Concr. Res. 97, 11–27. https://doi.org/10.1016/j.cemconres.2017.03.003.

Muñiz-Villarreal, M.S., Manzano-Ramírez, A., Sampieri-Bulbarela, S., Gasca-Tirado, J.R., Reyes-Araiza, J.L., Rubio-Ávalos, J.C., Pérez-Bueno, J.J., Apatiga, L.M., Zaldivar-Cadena, A., Amigó-Borrás, V., 2011. The effect of temperature on the geopolymerization process of a metakaolin-based geopolymer. Mater. Lett. 65, 995–998. https://doi.org/10.1016/j.matlet.2010.12.049.

NASA's Plan for Sustained Lunar Exploration and Development, 2020.

Naser, M.Z., 2019. Extraterrestrial construction materials. Prog. Mater. Sci. 105. https://doi.org/10.1016/j.pmatsci.2019.100577 100577.

Naser, M.Z., Chehab, A.I., 2020. Polymers in space exploration and commercialization, Polymer Science and Innovative Applications. INC. https://doi.org/10.1016/b978-0-12-816808-0.00014-7

Nath, P., Sarker, P.. ., 2012. Geopolymer concrete for ambient curing condition. Australas. Struct. Eng. Conf. 2012 past, Present Futur. Struct. Eng. 1–9.

Nath, P., Sarker, P.K., 2014. Effect of GGBFS on setting, workability and early strength properties of fly ash geopolymer concrete cured in ambient condition. Constr. Build. Mater. 66, 163–171. https://doi.org/10.1016/j.conbuildmat.2014.05.080.

Neves, J.M., Ramanathan, S., Suraneni, P., Grugel, R., Radlińska, A., 2020. Characterization, mechanical properties, and microstructural development of lunar regolith simulant-portland cement blended mixtures. Constr. Build. Mater. 258. https://doi.org/10.1016/j.conbuildmat.2020.120315 120315.

Nongnuang, T., Jitsangiam, P., Rattanasak, U., Tangchirapat, W., Suwan, T., Thongmunee, S., 2021. Characteristics of waste iron powder as a fine filler in a high-calcium fly ash geopolymer. Materials (Basel). 14, 1–15. https://doi.org/10.3390/ma14102515.

Ordonez, E., Edmunson, J., Fiske, M., Christiansen, E., Miller, J., Davis, B., Read, J., Johnston, M., Fikes, J., 2017. Hypervelocity impact testing of materials for additive construction: Applications on Earth, the Moon, and Mars. Procedia Eng. 204, 390–396. https://doi.org/10.1016/j.proeng.2017.09.787.

Palomo, Á., Alonso, S., Fernandez-Jiménez, A., Sobrados, I., Sanz, J., 2004. Alkaline activation of fly ashes: NMR study of the reaction products. J. Am. Ceram. Soc. 87, 1141–1145. https://doi.org/10.1111/j.1551-2916.2004.01141.x.

Palomo, A., Grutzeck, M.W., Blanco, M.T., 1999. Alkali-activated fly ashes: A cement for the future. Cem. Concr. Res. 29, 1323–1329. https://doi.org/10.1016/S0008-8846(98)00243-9.

Papike, J.J., Simon, S.B., Laul, J.C., 1982. The lunar regolith: Chemistry, mineralogy, and petrology. Rev. Geophys. 20, 761–826. https://doi.org/10.1029/RG020i004p00761.

Peters, G.H., Abbey, W., Bearman, G.H., Mungas, G.S., Smith, J.A., Anderson, R.C., Douglas, S., Beegle, L.W., 2008. Mojave Mars simulant-Characterization of a new geologic Mars analog. Icarus 197, 470–479. https://doi.org/10.1016/j.icarus.2008.05.004.

Phair, J.W., Van Deventer, J.S.J., 2002. Effect of the silicate activator pH on the microstructural characteristics of waste-based geopolymers. Int. J. Miner. Process. 66, 121–143. https://doi.org/10.1016/S0301-7516(02)00013-3.

Pilehvar, S., Arnhof, M., Pamies, R., Valentini, L., Kjøniksen, A.L., 2020. Utilization of urea as an accessible superplasticizer on the moon for lunar geopolymer mixtures. J. Clean. Prod. 247. https://doi.org/10.1016/j.jclepro.2019.119177.

Provis, J.L., 2018. Alkali-activated materials. Cem. Concr. Res. 114, 40–48. https://doi.org/10.1016/j.cemconres.2017.02.009.

Puertas, F., Martínez-Ramírez, S., Alonso, S., Vázquez, T., 2000. Alkali-activated fly ash/slag cements. Strength behaviour and hydration products. Cem. Concr. Res. 30, 1625–1632. https://doi.org/10.1016/S0008-8846(00)00298-2.

Puligilla, S., Mondal, P., 2013. Role of slag in microstructural development and hardening of fly ash-slag geopolymer. Cem. Concr. Res. 43, 70–80. https://doi.org/10.1016/j.cemconres.2012.10.004.

Rahier, H., Denayer, J.F., Van Mele, B., 2003. Low-temperature synthesized aluminosilicate glasses: Part IV. Modulated DSC study on the effect of particle size of metakaolinite on the production of inorganic polymer glasses. J. Mater. Sci. 38, 3131–3136. https://doi.org/10.1023/A:1024733431657.

Rahmatian, L.A., Metzger, P.T., 2010. Earth and Space 2010: Engineering, Science, Construction, and Operations in Challenging Environments - Proceedings of the 12th International Conference, in: Proceedings of the 12th International Conference on Engineering, Science, Construction, and Operations in Challenging Environments - Earth and Space 2010. pp. 239–253.

Ramkissoon, N.K., Pearson, V.K., Schwenzer, S.P., Schröder, C., Kirnbauer, T., Wood, D., Seidel, R.G.W., Miller, M.A., Olsson-Francis, K., 2019. New simulants for martian regolith: Controlling iron variability. Planet. Space Sci. 179. https://doi.org/10.1016/j.pss.2019.104722.

Ray, C.S., Reis, S.T., Sen, S., O'Dell, J.S., 2010. JSC-1A lunar soil simulant: Characterization, glass formation, and selected glass properties. J. Non. Cryst. Solids 356, 2369–2374. https://doi.org/10.1016/j.jnoncrysol.2010.04.049.

Reiter, L., Wangler, T., Roussel, N., Flatt, R., 2018. The role of early age structural build-up in digital fabrication with concrete. Cem. Concr. Res. (this issue). https://doi.org/10.1016/j.cemconres.2018.05.011.

Rickard, W.D.A., Van Riessen, A., Walls, P., 2010. Thermal character of geopolymers synthesized from class F Fly ash containing high concentrations of iron and α-quartz. Int. J. Appl. Ceram. Technol. 7, 81–88. https://doi.org/10.1111/j.1744-7402.2008.02328.x.

Rickard, W.D.A., Williams, R., Temuujin, J., van Riessen, A., 2011. Assessing the suitability of three Australian fly ashes as an aluminosilicate source for geopolymers in high temperature applications. Mater. Sci. Eng. A 528, 3390–3397. https://doi.org/10.1016/j.msea.2011.01.005.

Roussel, N., 2018. Rheological requirements for printable concretes. Cem. Concr. Res. 1–10. https://doi.org/10.1016/j.cemconres.2018.04.005.

Roussel, N., Ovarlez, G., Garrault, S., Brumaud, C., 2012. The origins of thixotropy of fresh cement pastes. Cem. Concr. Res. 42, 148–157. https://doi.org/10.1016/j.cemconres.2011.09.004.

Rouyer, J., Poulesquen, A., 2015. Evidence of a Fractal Percolating Network During Geopolymerization. J. Am. Ceram. Soc. 98, 1580–1587. https://doi.org/10.1111/jace.13480.

Rovnaník, P., 2010. Effect of curing temperature on the development of hard structure of metakaolin-based geopolymer. Constr. Build. Mater. 24, 1176–1183. https://doi.org/10.1016/j.conbuildmat.2009.12.023.

Sanders, G.B., Larson, W.E., 2012. Progress made in lunar in-situ resource utilization under NASA's exploration technology and development program. Earth Sp. 2012 - Proc. 13th ASCE Aerosp. Div. Conf. 5th NASA/ASCE Work. Granul. Mater. Sp. Explor. 457–478. https://doi.org/10.1061/9780784412190.050

Scott, A.N., Oze, C., Tang, Y., O'Loughlin, A., 2017. Development of a Martian regolith simulant for in-situ resource utilization testing. Acta Astronaut. 131, 45–49. https://doi.org/10.1016/j.actaastro.2016.11.024.

Seedhouse, E., 2013. Falcon 9 and Falcon Heavy: Life after the Space Shuttle, in: SpaceX: Making Commercial Spaceflight a Reality. Springer, pp. 65–84. https://doi.org/10.1007/978-1-4614-5514-1_5

Shi, C., Jiménez, A.F., Palomo, A., 2011. New cements for the 21st century: The pursuit of an alternative to Portland cement. Cem. Concr. Res. 41, 750–763. https://doi.org/10.1016/j.cemconres.2011.03.016.

Sibille, L., Carpenter, P., Schlagheck, R., French, R., 2006. Lunar Regolith Simulant Materials: Recommendations for Standardization, Production, and Usage. NASA Tech, Pap, p. 142.

Sindhunata, Van Deventer, J.S.J., Lukey, G.C., Xu, H., 2006. Effect of curing temperature and silicate concentration on fly-ash-based geopolymerization. Ind. Eng. Chem. Res. 45, 3559–3568. https://doi.org/10.1021/ie051251p

Singh, N.B., Middendorf, B., 2020. Geopolymers as an alternative to Portland cement: An overview. Constr. Build. Mater. 237. https://doi.org/10.1016/j.conbuildmat.2019.117455 117455.

SpaceX, 2021. Falcon Heavy [WWW Document]. URL https://www.spacex.com/vehicles/falcon-heavy/

Stoeser, D.B., Rickman, D.L., Wilson, S. a., 2010. Preliminary Geological Findings on the BP-1 Simulant. Nasa Tm 24.

Sturm, P., Gluth, G.J.G., Simon, S., Brouwers, H.J.H., Kühne, H.C., 2016. The effect of heat treatment on the mechanical and structural properties of one-part geopolymer-zeolite composites. Thermochim. Acta 635, 41–58. https://doi.org/10.1016/j.tca.2016.04.015.

Su, H., Hong, Y., Chen, T., Kou, R., Wang, M., Zhong, Y., Qiao, Y., 2019. Fatigue Behavior of Inorganic-Organic Hybrid "Lunar Cement". Sci. Rep. 9, 1–8. https://doi.org/10.1038/s41598-019-38799-x.

Suescun-Florez, E., Roslyakov, S., Iskander, M., Baamer, M., 2015. Geotechnical properties of BP-1 lunar regolith simulant. J. Aerosp. Eng. 28, 1–9. https://doi.org/10.1061/(ASCE)AS.1943-5525.0000462.

Swanepoel, J.C., Strydom, C. a., 2002. Utilisation of fly ash in a geopolymeric material. Appl. Geochemistry 17, 1143–1148.

Toutanji, H.A., Evans, S., Grugel, R.N., 2012. Performance of lunar sulfur concrete in lunar environments. Constr. Build. Mater. 29, 444–448. https://doi.org/10.1016/j.conbuildmat.2011.10.041.

Walton, R.I., Millange, F., O'Hare, D., Davies, A.T., Sankar, G., Catlow, C.R.A., 2001. In situ energy-dispersive X-ray diffraction study of the hydrothermal crystallization of zeolite A. 1. Influence of reaction conditions and transformation into sodalite. J. Phys. Chem. B 105, 83–90. https://doi.org/10.1021/jp002711p.

Wan, L., Wendner, R., Cusatis, G., 2016. A novel material for in situ construction on Mars: experiments and numerical simulations. Constr.

Build. Mater. 120, 222–231. https://doi.org/10.1016/j.conbuildmat.2016.05.046.

Wang, K. tuo, Lemougna, P.N., Tang, Q., Li, W., Cui, X. min, 2017. Lunar regolith can allow the synthesis of cement materials with near-zero water consumption. Gondwana Res. 44, 1–6. https://doi.org/10.1016/j.gr.2016.11.001

Wang, K.T., Tang, Q., Cui, X.M., He, Y., Liu, L.P., 2016. Development of near-zero water consumption cement materials via the geopolymerization of tektites and its implication for lunar construction. Sci. Rep. 6, 1–8. https://doi.org/10.1038/srep29659.

Werkheiser, N.J., Fiske, M.R., Edmunson, J.E., Khoshnevis, B., 2015. Development of additive construction technologies for application to development of lunar/martian surface structures using in-situ materials. CAMX 2015 - Compos. Adv. Mater. Expo 2395–2402.

White, A.F., Brantley, S.L., 2003. The effect of time on the weathering of silicate minerals: Why do weathering rates differ in the laboratory and field? Chem. Geol. 202, 479–506. https://doi.org/10.1016/j.chemgeo.2003.03.001.

Wilhelm, S., Curbach, M., 2014. Review of possible mineral materials and production techniques for a building material on the moon. Struct. Concr. 15, 419–428. https://doi.org/10.1002/suco.201300088.

Williams, J.P., Paige, D.A., Greenhagen, B.T., Sefton-Nash, E., 2017. The global surface temperatures of the moon as measured by the diviner lunar radiometer experiment. Icarus 283, 300–325. https://doi.org/10.1016/j.icarus.2016.08.012.

Yusuf, M.O., 2015. Performance of slag blended alkaline activated palm oil fuel ash mortar in sulfate environments. Constr. Build. Mater. 98, 417–424. https://doi.org/10.1016/j.conbuildmat.2015.07.012.

Zeng, X., He, C., Oravec, H., Wilkinson, A., Agui, J., Asnani, V., 2010. Geotechnical Properties of JSC-1A Lunar Soil Simulant. J. Aerosp. Eng. 23, 111–116. https://doi.org/10.1061/(asce)as.1943-5525.0000014.

Zhang, H., Xu, Y., Gan, Y., Chang, Z., Schlangen, E., Šavija, B., 2020a. Microstructure informed micromechanical modelling of hydrated cement paste: Techniques and challenges. Constr. Build. Mater. 251. https://doi.org/10.1016/j.conbuildmat.2020.118983 118983.

Zhang, P., Gao, Z., Wang, J., Guo, J., Hu, S., Ling, Y., 2020b. Properties of fresh and hardened fly ash/slag based geopolymer concrete: A review. J. Clean. Prod. 270. https://doi.org/10.1016/j.jclepro.2020.122389 122389.

Zhang, Z., Provis, J.L., Wang, H., Bullen, F., Reid, A., 2013. Quantitative kinetic and structural analysis of geopolymers. Part 2. Thermodynamics of sodium silicate activation of metakaolin. Thermochim. Acta 565, 163–171. https://doi.org/10.1016/j.tca.2013.01.040.

Zhang, Z., Wang, H., Provis, J.L., Bullen, F., Reid, A., Zhu, Y., 2012. Quantitative kinetic and structural analysis of geopolymers. Part 1. the activation of metakaolin with sodium hydroxide. Thermochim. Acta 539, 23–33. https://doi.org/10.1016/j.tca.2012.03.021.

Zhou, S., Lu, C., Zhu, X., Li, F., 2020. Preparation and characterization of high-strength geopolymer based on BH-1 lunar soil simulant with low alkali content. Engineering. https://doi.org/10.1016/j.eng.2020.10.016.